Proceedings of ASME 2016 International Mechanical Engineering Congress and Exposition
IMECE2016
November 11-17, 2016, Phoenix, Arizona, USA

IMECE2016-65954

WIRELESS INTERROGATION OF A HIGH TEMPERATURE ANTENNA SENSOR WITOUTH ELECTRONICS

Jun Yao
Dept.of Electrical Eng.
University of Texas at Arlington
Arlington,TX, USA

Franck Mbanya Tchafa
Dept. of Mechanical and Aerospace Eng.
University of Texas at Arlington
Arlington,TX, USA

Haiying Huang
Dept. of Mechachinal and Aerospace Eng.
University of Texas at Arlington
Arlington,TX, USA

ABSTRACT

This paper presents a novel interrogation mechanism for an antenna sensor subjected to high temperatures. In sensor node, an Ultra-wide Band (UWB) microstrip antenna was used as a wireless Tx/Rx transceiver to amplify the reflected interrogation signal from the temperature-sensing element, i.e. the patch antenna-sensor. A microstrip delay line was used to connect the Tx/Rx antenna and the antenna-sensor so that the reflected signal from the sensor node is delayed and can be separated from the background clutter using time-domain (T-D) gating technique. In this paper, the operation principle of the proposed interrogation mechanism is first discussed, followed by the design and simulations of the sensor node circuitry. Finally, a temperature test was conducted to validate the wireless temperature sensing performance of the antenna sensor.

INTRODUCTION

Microstrip antennas are widely used as sensors due to their low cost, compact size, passive operation and multi-modality sensitivity [1]-[2]. As a promising sensor, its sensing ability for temperature, mechanical stress and crack has been demonstrated [3]-[5]. Because of its simple and conformal planar configuration, a patch antenna-sensor can be easily attached on the structure surface for Structure Health Monitoring (SHM) [1]. By detecting the resonant frequency shift of the antenna-sensor, the structure physical properties can be determined. In the aspect of wireless interrogation, an antenna-sensor can be wirelessly interrogated at middle range distances without an on-board battery [4]. However, this passive wireless antenna sensor has to have a transistor. Therefore, it cannot used for temperature beyond the temperature limitation of the transistor.

A typical psddivr wireless sensor system contains two parts: the wireless interrogator and the wireless sensor node [4], [6]. An interrogation signal is first broadcasted to the sensor node from the wireless interrogator [4], [7]-[8]. Once the interrogation signal is received by the sensor node, sensing information is encoded in the received signal. Subsequently, the encoded signal is re-transmitted back so that the wireless interrogator can retrieve the sensing information. Since the backscattered signal also contains background clutter, it creates the "self-jamming" problem [1]. How to separate the antenna backscattering from the background clutter becomes a major challenge. Several wireless interrogation techniques that address this self-jamming problem have been developed. One of the approaches is to modulate the amplitude of the antenna backscattering [3]. Wireless interrogation system that uses the radio-frequency identification (RFID) technology has also been demonstrated [9]. However, because of the temperature limitation of the electric components at the sensor-node, the antenna backscattering modulation scheme and the RFID-based interrogation are only suitable for low temperature environment. In order to use the antenna-sensor in harsh environment, new sensor architecture should be designed without electronics. In Cheng's paper [10], a near-field T-D gating interrogation approach was proposed. In his research, in order to minimize the background clutter, a patch antenna-sensor was wirelessly interrogated using an open-ended waveguide (OEWG) at a short distance. Because of the small

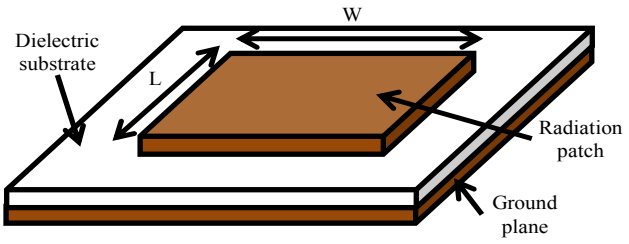

Fig. 1. Illustration of a microstrip patch antenna

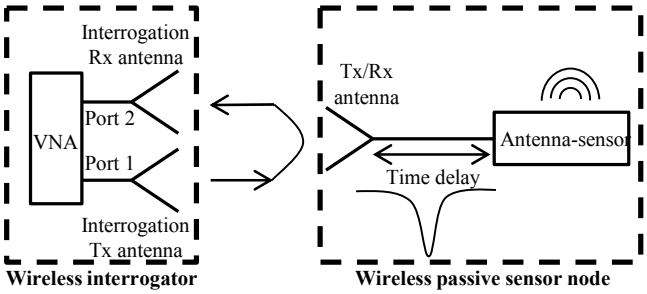

Fig. 2. Block diagram of the wireless interrogation system

OEWG aperture and the short interrogation distance the amplitude of the background clutter is minimized. T-D gate was used to capture the radiating signal form the antenna-sensor only to get its resonance frequency [11], [12]. Since the patch-antenna is not a perfect resonator [13] its Quality (Q) factor is limited to 100. The wireless interrogation distance of this mechanism is only 5 cm.

In this study, a wireless interrogation system suitable for high temperature sensing was developed. Different from the techniques mentioned above, a patch antenna-sensor was implemented at the senor node for temperature sensing. An UWB high gain antenna [14]-[15] was added and served as a passive wireless transceiver for the antenna-sensor. Instead of capturing the antenna-sensor's radiating signal, the reflected signal from the antenna-sensor was radiated through the UWB Tx/Rx antenna to the interrogator. At the interrogator side, T-D gating technique was used to separate the Tx/Rx antenna backscattering from the background clutter, and retrieve the real-time antenna-sensor's resonant frequency from its reflection coefficient. Since all the components at the sensor node are microstrip based, the proposed sensor-node circuitry can be used in harsh environment that can be tolerated by the high-temperature Printed Circuit Board (PCB) material.

PRINCIPLE OF OPERATION

A. Patch antenna for temperature sensing

Microstrip patch antenna has been proven for temperature sensing using wired connections [3]. By detecting the shift of the antenna resonant frequency, the temperature variation can be determined based on the linear relationship between them. For a rectangular patch antenna, which is operating in TM_{010} mode as shown in Figure 1, the resonant frequency f_{res} can be calculated using the following equation [16]:

$$f_{res} = \frac{C}{2L\sqrt{\varepsilon_r}}, \quad (1)$$

where C is the light of speed; L is the physical length of the patch antenna and ε_r if the dielectric constant of the substrate material.

The resonant frequency variation δf_{res} can then be expressed in terms of the changes in the substrate dielectric constant ε_r and the patch length L, which can be expressed as

$$\delta f_{res} = \frac{\partial f_{res}}{\partial \varepsilon_r}\delta\varepsilon_r + \frac{\partial f_{res}}{\partial L}\delta L. \quad (2)$$

From equation (1) we can also derive that

$$\frac{\partial f_{res}}{\partial \varepsilon_r} = \left(-\frac{1}{2\varepsilon_r}\right) f_{res} \quad (3)$$

and

$$\frac{\partial f_{res}}{\partial L} = \left(-\frac{1}{L}\right) f_{res}. \quad (4)$$

Substituting (3), (4) into (2) and normalizing the shift of resonant frequency with the antenna's initial resonant frequency, we obtain:

$$\frac{\delta f_{res}}{f_{res}} = -\frac{1}{2}\frac{\delta\varepsilon_r}{\varepsilon_r} - \frac{\delta L}{L}. \quad (5)$$

For the purpose of temperature sensing equation (5) can be converted into another form

$$\frac{\delta f_{res}}{f_{res}} = -\frac{1}{2}\alpha_\varepsilon \delta T - \alpha_T \delta T = \left(-\frac{1}{2}\alpha_\varepsilon - \alpha_T\right)\delta T = K_T \delta T, \quad (6)$$

where α_ε is the thermal coefficient of substrate dielectric constant; α_T is the coefficient for material thermal expansion; δT stands for temperature variation; K_T is defined as the temperature sensitivity of the normalized frequency shift and is a linear function of α_ε and α_T. K_T will remain the same if α_ε and α_T of the substrate material are constants.

B. Wireless interrogation based on time-gate technology

1) Hardware setup for wireless interrogation system

A microstrip patch antenna-sensor was used for temperature sensing, and a wireless antenna interrogation system was setup to detect the antenna-sensor's resonant frequencies at different temperatures. The block diagram of the temperature sensing system is shown in Figure 2. It can be separated into two parts: the wireless interrogator and wireless passive sensor node. In the interrogator side, two broadband interrogation antennas are connected with a Vector Network Analyzer (VNA). These broadband interrogation antennas serve as wireless transmitter and receiver for the interrogator, respectively. The VNA first sends an FMCW interrogation signal to the Tx antenna, which is used to broadcast the signal to the sensor node. The reflected interrogation signal is received by the Rx antenna and collected by the VNA so that S21 parameters are recorded for every

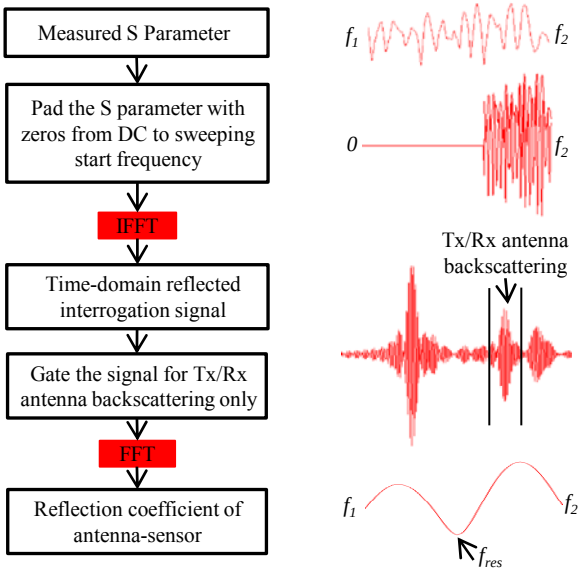

Fig. 3. Simulated relationship between the antenna-sensor's resonant frequency and dielectric constant of the substrate

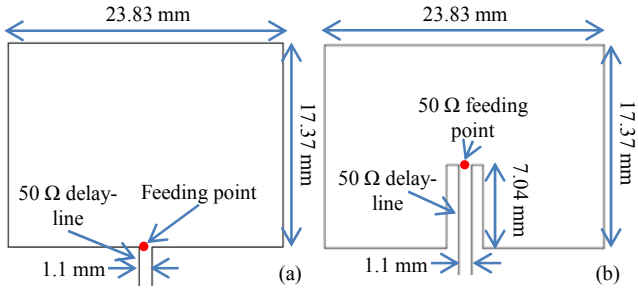

Fig. 3. Microstrip antenna-sensor (a) edge fed (b) inset fed.

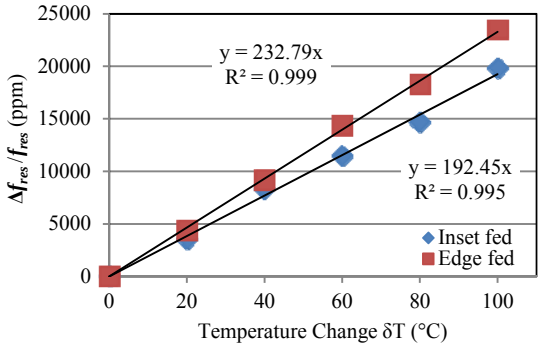

Fig. 4. Simulated relationship between the antenna-sensor's normalized resonant frequency shift and the temperature change.

interrogation. At the sensor node, an UWB Tx/Rx antenna is developed as the wireless transceiver. In the interrogation frequency range the designed Tx/Rx antenna has a high radiation gain. The high gain ensures the backscattered signal has a sufficient Signal to Noise Ratio (SNR). The wide band interrogation signal captured by the Tx/Rx antenna is sent to the antenna-sensor via a long microstrip delay line. The RF energy at the antenna resonant frequency is radiated by the antenna-sensor, and the remaining interrogation energy is reflected back to the Tx/Rx antenna by following the same delay line. As such, the reflection coefficient of the antenna-sensor is encoded into the Tx/Rx antenna backscattering. Due to the round trip transmission on the delay line, the Tx/Rx antenna backscattering has a specific time delay. Therefore, it can be easily distinguished from the background clutter using a Digital Signal Program (DSP) that performs time-gating and frequency analysis of the received signal.

2) Software DSP for Wireless interrogation

The logic flow chart of the DSP is represented in Figure 3. First, the frequency of the S21 parameter ranges from f_1 to f_2 and thus it is zero padded from DC (0 Hz) to f_1. The padded S parameter is then converted to a time-domain signal using Inverse Fast Fourier Transform (IFFT) [17]. The starting and ending time of the antenna backscattering are then identified and the signal fall within the time window is time gated. Subsequently, the gated sensor node signal is transferred back to the frequency domain using Fast Fourier Transform (FFT). The resonant frequency of the antenna-sensor can then be determined as the frequency that has the lowest reflection coefficient.

SENSOR NODE IMPLEMENTATION

A. *Design of temperature antenna-sensor*

Rogers RO3210 [18] was selected as the antenna substrate because of its high thermal coefficient of dielectric constant α_ε, which is -459 ppm/°C in the temperature range from 0°C to 100°C. Compare to α_ε, the thermal expansion coefficient α_T of the material is much lower, which is only 13 ppm/°C in the temperature range from -55°C to 288°C. Therefore, the effect of α_T on the antenna-senosr's resonant frequency is ignored and the theoretical temperature sensitivity of the normalized frequency shift K_T can be calculated as 225.9 ppm/°C. A rectangular patch antenna resonating at 2.5 GHz was fabricated using Rogers laminate RO3210. A 3D model of the designed antenna-sensor was developed in HFSS and EM simulations were performed. Two feeding structures were used during the simulations. The first one is edge feeding, as shown in Figure 3(a); the feeding point was located in the middle of the patch's bottom edge. As such, the patch shape can be maintained but the reflection coefficient will be high at antenna's resonant frequency because of the impedance mismatch between edge feeding point and 50 Ω transmission delay line. In order get lower reflection coefficient, inset fed technology was also used. The 50 Ω feeding point was calculated at the position of 7.04 mm above the bottom edge of the patch as shown in Figure 3(b). Consider the substrate's dielectric constant is 10.8 at room temperature (20°C), it means it will reduce 10.8 * (-459) ppm/°C * 20 °C = 0.1 for every 20 °C of temperature increase. Thus, during the simulations, the substrate dielectric constant

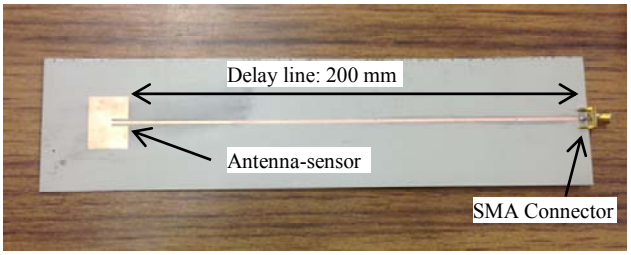

Fig. 5. Fabricated antenna-senor and delay line

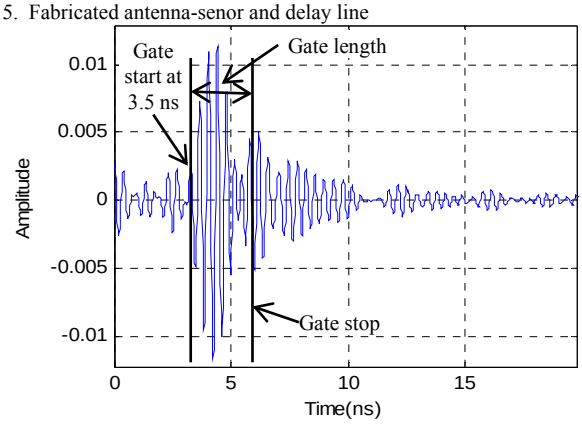

Fig. 6. Time domain response converted from S11 parameter

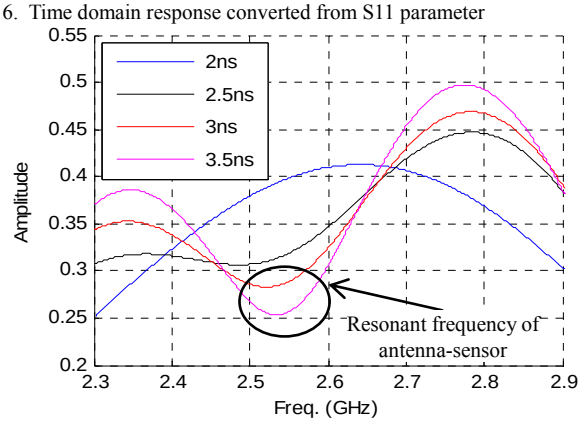

Fig. 7. FFT of the gated T-D signal

was swept from 10.9 to 10.4 with a step of -0.1 in order to simulate the temperature from 0 to 100 °C with an increment of 20 °C. From the simulated results presented in Figure 4, the simulated temperature sensitivity K_T, is 232.79 ppm/°C which agrees well with the theoretical value of 225.9 ppm/°C. The simulated K_T for the patch with an inset slot gap is lower which is 195.42 ppm/°C. Considering the good linearity (R^2 = 0.995) and the better impedance matching, the inset fed structure was used in this study.

A 200 mm microstrip transmission delay line which has a characteristic impedance of 50 Ω was designed to feed the antenna-sensor. As shown in figure 3(a), one end of the feeding line was connected with the 50 Ω feeding point and the width of the transmission line is 1.1 mm. The antenna-sensor and the delay line were fabricated using a chemical etching technique, as shown in Figure 5. In Figure 6, due to the delay line, the

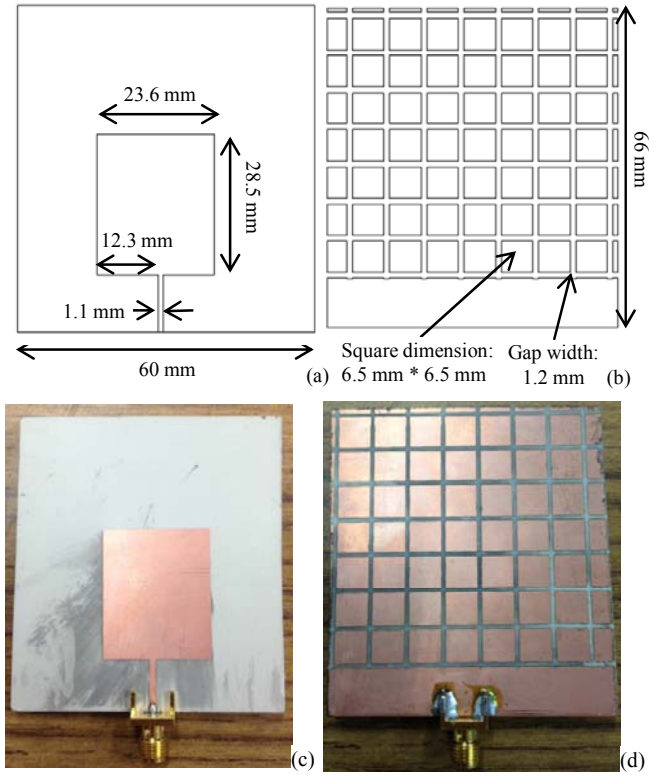

Fig. 8. UWB Tx/Rx antenna (a) dimension of the front side (b) dimension of the back side (c) front side of the fabricated antenna (d) back side of the fabricated antenna

reflected signal from the antenna-sensor starts at around 3.5 ns. Therefore the T-D gate starting point is set as 3.5 ns and different gate lengths were selected to gate the antenna-sensor signal. Figure 7 shows that if the gate length is longer than 3 ns, we can determine the antenna-sensor's resonant frequency from the FFT of the gated signal.

B. Design of UWB Tx/Rx microstrip antenna

In order to wirelessly capture the wide-band FMCW interrogation signal, a high gain UWB antenna was developed. The Tx/Rx antenna configuration is based on a one-layer patch antenna using the same PCB material as that of the antenna-sensor, i.e. Rogers laminate RO3210. The top layer of the designed interrogation antenna is a regular patch which has the lowest resonant frequency of 1.6 GHz. The physical dimension of the patch is shown in Figure 8(a). A 50 Ω transmission line with a width of 1.1 mm was used to feed the antenna. Different from a regular patch antenna, periodically distributed cross strip-line gaps are designed on the ground layer of this Tx/Rx antenna. As shown in Figure 8(b), the strips separate the ground plane into small squares which have the dimension of 6.5 mm* 6.5 mm. The strip-gap added to the ground together with the radiation patch above can be considered as a type of metamaterial structure - Reactive impedance Surface (RIS).

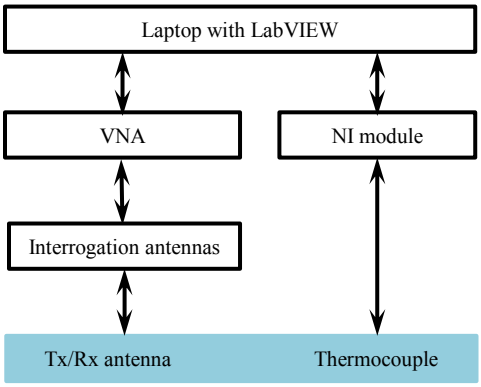

Fig. 11. Block diagram for DAQ system

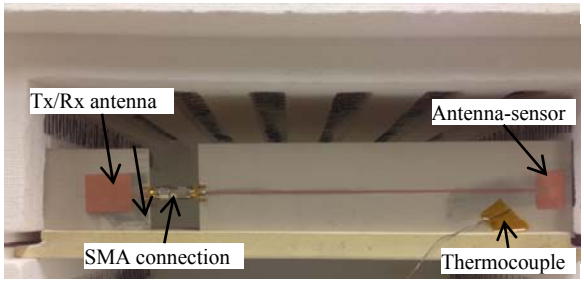

Fig. 12. Sensor node circuitry for low-temperature testing

The RIS metamaterial is employed to broaden the resonant frequencies and enhance the radiation performance of the antenna via reactive coupling with the patch and the substrate. The Tx/Rx antenna's performance was firstly simulated using HFSS. The antenna was fabricated which is represented in Figure 8(c) and 8(d) using chemical etching and the S11 curve was measured to validate the simulation results. As seen from Figure 9, the measured bandwidth where the reflection coefficient is less than -10 dB ranges is from 1.9 to 3.5 GHz. This matches with the simulation very well. Compare to the regular patch antenna, which has the same patch dimension, the -10 dB operation bandwidth of the proposed antenna increases more than 100 times. This is because the magnetic energy stored in RIS structure compensates for the electrical energy stored in the near field of the patch antenna, which results in the additional resonance at lower frequency.

In order to characterize the antenna radiation performance, the gain of the Tx/Rx antenna was measured at different operation frequencies. As seen from the measurement results shown in Figure, the gain of the designed antenna is relative stable, which verifies from 3.2 to 4 dB in the frequency range from 2 to 3 GHz.

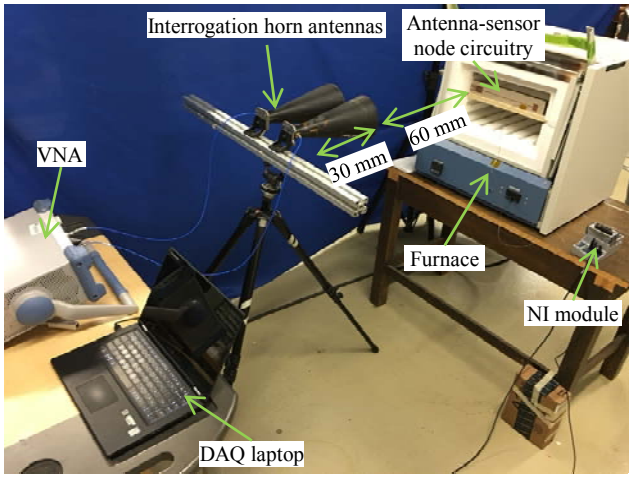

Fig. 11. System setup for temperature testing

EXPERIMENTAL SETUP

The experimental setup of the wireless temperature sensing system is showed in Figure 11. In this setup, a furnace was used as the heat source. The door of the furnace was removed for wireless interrogation of the sensor node circuitry, which was placed at the furnace entrance. A T-type thermocouple was placed adjacent to the antenna-sensor to obtain the reference temperature. Data from the thermocouple were acquired using National Instruments (NI) thermocouple module that provides cold-junction-compensation and linearization. Two interrogation horn antennas were set in front of the Tx/Rx antenna with an interrogation distance of 60 cm. Using two coaxial cables, the horns antennas were connected to a VNA for the acquisition of scattering (S) parameters. The distance between the VNA feeding point and the aperture of the interrogation horn antenna is 30 cm. Therefore, the wireless transmission distance between the feed point and Tx/Rx antenna is 30 cm + 60 cm = 90 cm.

The arrival time for the signal backscattered by the antenna sensor can be calculated as following:

$$T_{start} = D_{air} + D_{delay} , \quad (7)$$

where D_{air} is the time spent on the round-trip wireless transmission between the interrogator and the Tx/Rx antenna; D_{delay} is the time delay caused by the microstrip delay line in antenna-sensor node. Since the wireless transmission distance is 0.9 m and the velocity of the EM wave in the air is the speed of light (3e8 m/s), D_{air} is 6 ns and D_{delay} is measured as 3.5 ns. Therefore, the T_{start} for this setup is 9.5 ns.

Both the reference temperature data from thermocouple and the S parameters from VNA were collected by a laptop using LavVIEW program. The flow diagram of the DAQ system is shown in Figure 11. The VNA was calibrated to the end of the coaxial cable and programmed to acquire S21 parameters with a frequency resolution of 200 kHz over a specified frequency range of 2.2 to 3 GHz using a 10 dbm interrogation power. During the entire experiment, the LabVIEW program simultaneously collected the S21 parameters and the thermocouple readings. The thermocouple readings were recorded every 0.1 second while the S21 parameters were recorded every 2.3 seconds. Both recorded data were time stamped for easily correlation between the thermocouple readings and the extracted resonant frequency from the S21 parameters.

RESULTS AND DISCUSSION

In order to validate the proposed wireless interrogation mechanism, the Tx/Rx antenna and the antenna-sensor are fabricated on different boards using the same PCB material, i.e. Rogers laminate RO3210, and connected with each other using SMA connectors (See Figure 12). Due to the SMA connectors, the testing temperature range was set from 35 to 100 °C. During the tests, S21 were recorded at different testing temperatures and converted into T-D signals. The converted T-D signal for 35 °C is shown in Figure 12. The first wave packet is the result of the coupling between the two interrogation horn antennas. The second wave packet is the result of the background clutter from the system setup. It starts at around 6 ns and ends at 9 ns. Due to time delay caused by the microstrip delay line, the Tx/Rx antenna backscattering can be distinguished from background clutter in time domain. As shown in Figure 11, the Tx/Rx antenna backscattering starts around 9.5 ns, which matches perfectly with the calculated value discussed previously. Therefore, time-gating from 9.5 ns to 12.5 ns was applied on the T-D signal to cut the Tx/Rx antenna backscattering only. After T-D gating, the gated signals were converted back to the frequency domain in order to get the reflection coefficients of the antenna-sensor. The FFT of the gated signals at different temperatures are represented in Figure 14. As seen from Figure 14, antenna-sensor's reflection coefficient curve shifts to the right as temperature increasing. The resonant frequencies of the antenna-sensor can be found at the position that has the lowest reflection coefficient. The frequency shifts at different temperatures were measured and normalized with respect to the resonant frequency of the antenna-sensor at 35 °C. In Figure 15, the normalized frequency shifts are plotted versus the temperature change measured from the thermocouple. The experimental curve displayed a high degree of linearity (coefficient of determination R^2 = 0.9972). The measured temperature sensitivity of the normalized frequency shift k_T is 188.65

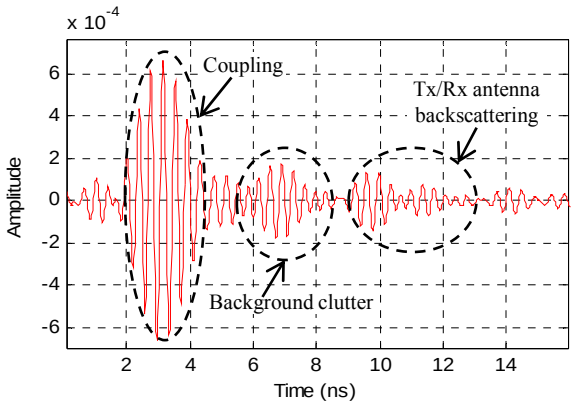

Fig. 13. Time domain reflection signal converted from S21 parameter

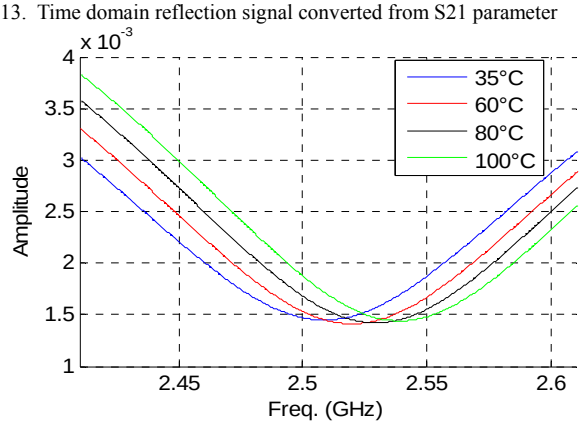

Fig. 14. FFT of gated T-D signal at different temperatures

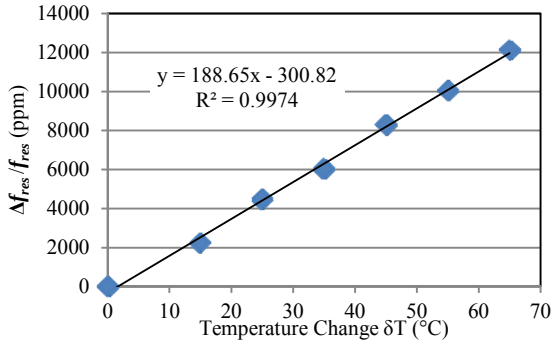

Fig. 15. Measured relationship between the antenna-sensor's normalized resonant frequency shift and the temperature change from low temperature testing

ppm/°C which is in good agreement with the simulated value, i.e. 192.45 ppm/°C.

CONCLUSION

In this paper, a wireless antenna temperature sensor without any electronics on board is presented. Since all the components in the sensor node are microstrip circuits, it can be implemented for temperature sensing in harsh environment. The proposed wireless interrogation system works at the far-field of the interrogation antenna and 60 cm interrogation distance is achieved. Temperature testing was conducted to

validate the accuracy of the designed interrogation system. The measured temperature sensing resolution is 188.65 ppm/°C which is 1.9% higher than the simulated value. A high-temperature PCB material will be developed to achieve higher temperature wireless sensing.

ACKNOWLEDGMENTS

This material is based upon work supported by the Department of Energy under Award Number DE-FE0023118. This report was prepared as an account of work sponsored by an agency of the United States Government. Neither the United States Government nor any agency thereof, nor any of their employees, makes any warranty, express or implied, or assumes any legal liability or responsibility for the accuracy, completeness, or usefulness of any information, apparatus, product, or process disclosed, or represents that its use would not infringe privately owned rights. Reference herein to any specific commercial product, process, or service by trade name, trademark, manufacturer, or otherwise does not necessarily constitute or imply its endorsement, recommendation, or favoring by the United States Government or any agency thereof. The views and opinions of authors expressed herein do not necessarily state or reflect those of the United States Government or any agency thereof.

REFERENCES

[1] H. Huang. Flexible wireless antenna sensor: A review. *Sensors Journal, IEEE 13(10),* pp. 3865-3872. 2013.

[2] A. Deivasigamani, A. Daliri, C. H. Wang and S. John. A review of passive wireless sensors for structural health monitoring. *Modern Applied Science 7(2),* pp. 57. 2013.

[3] J. W. Sanders, J. Yao and H. Huang. Microstrip patch antenna temperature sensor. *Sensors Journal, IEEE 15(9),* pp. 5312-5319. 2015.

[4] J. Yao, S. Tjuatja and H. Huang. Real-time vibratory strain sensing using passive wireless antenna sensor. 2013.

[5] I. Mohammad and H. Huang. An antenna sensor for crack detection and monitoring. *Adv. Struct. Eng. 14(1),* pp. 47-53. 2011.

[6] J. Yao, Y. Hew, A. Mears and H. Huang. Strain gauge-enable wireless vibration sensor remotely powered by light.

[7] C. Li, W. Chen, G. Liu, R. Yan, H. Xu and Y. Qi. A noncontact FMCW radar sensor for displacement measurement in structural health monitoring. *Sensors 15(4),* pp. 7412-7433. 2015.

[8] S. Deshmukh and H. Huang, "Wireless interrogation of passive antenna sensors." *Measurement Science and Technology*, vol. 21, no. 3, p. 035201, 2010.

[9] X. Yi, C. Cho, J. Cooper, Y. Wang, M. M. Tentzeris and R. T. Leon. Passive wireless antenna sensor for strain and crack sensing—electromagnetic modeling, simulation, and testing. *Smart Mater. Struct.22(8),* pp. 085009. 2013.

[10] H. Cheng, S. Ebadi, X. Ren and X. Gong. Wireless passive high-temperature sensor based on multifunctional reflective patch antenna up to 1050 degrees centigrade. Sensors and Actuators A: Physical 222 pp. 204-211. 2015.

[11] H. Cheng, S. Ebadi and X. Gong. A low-profile wireless passive temperature sensor using resonator/antenna integration up to 1000 C. *Antennas and Wireless Propagation Letters, IEEE 11*pp. 369-372. 2012.

[12] D. Thomson, D. Card and G. Bridges. RF cavity passive wireless sensors with time-domain gating-based interrogation for SHM of civil structures. *Sensors Journal, IEEE 9(11),* pp. 1430-1438. 2009.

[13] A. Daliri, A. Galehdar, W. S. Rowe, S. John, C. H. Wang and K. Ghorbani. Quality factor effect on the wireless range of microstrip patch antenna strain sensors. *Sensors 14(1),* pp. 595-605. 2014.

[14] H. Mosallaei and K. Sarabandi. Antenna miniaturization and bandwidth enhancement using a reactive impedance substrate. *Antennas and Propagation, IEEE Transactions on 52(9),* pp. 2403-2414. 2004.

[15] L. Li, Y. Li, T. S. Yeo, J. R. Mosig and O. J. Martin. A broadband and high-gain metamaterial microstrip antenna. *Appl. Phys. Lett. 96(16),* pp. 164101. 2010.

[16] Balanis C, *Antenna Theory Analysis and Design*, 3rd ed. New York: Wiley Interscience, 2005.

[17] H. Huang and T. Bednorz. Introducing S-parameters for ultrasound-based structural health monitoring. *Ultrasonics, Ferroelectrics, and Frequency Control, IEEE Transactions on 61(11),* pp. 1856-1863. 2014.

[18] Rogers Corporation. (2011). RO3000 Series Circuit Materials Datasheet. [Online].